Multimodal Fusion Strategies for Outcome Prediction in Stroke

Esra Zihni[1,3] [a], Vince Madai[1], Ahmed Khalil[2], Ivana Galinovic[2], Jochen Fiebach[2] [b],
John D. Kelleher[3] [c], Dietmar Frey[1] and Michelle Livne[1]

[1]*Predictive Modelling in Medicine Research Group, Department of Neurosurgery,
Charité - Universitätsmedizin Berlin, Berlin, Germany*
[2]*Centre for Stroke Research Berlin, Charité - Universitätsmedizin Berlin, Berlin, Germany*
[3]*ADAPT Research Center, Technological University Dublin, Dublin, Ireland*

Keywords: Machine Learning, Multimodal Fusion, Neural Networks, Predictive Modeling, Acute-ischemic Stroke.

Abstract: Data driven methods are increasingly being adopted in the medical domain for clinical predictive modeling. Prediction of stroke outcome using machine learning could provide a decision support system for physicians to assist them in patient-oriented diagnosis and treatment. While patient-specific clinical parameters play an important role in outcome prediction, a multimodal fusion approach that integrates neuroimaging with clinical data has the potential to improve accuracy. This paper addresses two research questions: (a) does multimodal fusion aid in the prediction of stroke outcome, and (b) what fusion strategy is more suitable for the task at hand. The baselines for our experimental work are two unimodal neural architectures: a 3D Convolutional Neural Network for processing neuroimaging data, and a Multilayer Perceptron for processing clinical data. Using these unimodal architectures as building blocks we propose two feature-level multimodal fusion strategies: 1) extracted features, where the unimodal architectures are trained separately and then fused, and 2) end-to-end, where the unimodal architectures are trained together. We show that integration of neuroimaging information with clinical metadata can potentially improve stroke outcome prediction. Additionally, experimental results indicate that the end-to-end fusion approach proves to be more robust.

1 INTRODUCTION

Stroke[1] is a major cause of death and long-term disabilities worldwide. In the clinical setting, physicians decide which patients will benefit from treatment on the basis of likely long-term outcomes if treated. Currently, a time-window approach based on the time from stroke onset to treatment is being used as the main treatment decision criteria, together with subjective assessment of acute stroke imaging acquired in routine examination. Outcome prediction in stroke aims to develop a machine learning based decision support system that provides reliable information to physicians to assist them for better diagnosis and treatment for ischemic stroke patients. It is known that patient-specific clinical parameters play an important role in creating a baseline for outcome prediction, while combining imaging information has the potential to improve the predictive accu-

racy (Asadi et al., 2014; Whiteley et al., 2012; Vora et al., 2011). We hypothesize that using state-of-the-art machine learning algorithms to train a model on both data modalities (i.e. clinical metadata and neuroimaging) would increase outcome prediction accuracy. We aim to develop an automated method to predict a binary 3 months post-stroke outcome, using time-of-flight (TOF) magnetic resonance angiography (MRA) images and clinical metadata.

Deep learning methods have achieved state-of-the-art performance compared to classical machine learning methods in predictive modeling, which has led to their increased adoption in medical applications (Kelleher, 2019). A number of studies have presented models using Multilayer Perceptrons (MLPs) for outcome prediction based on clinical parameters (Asadi et al., 2014; Heo et al., 2019). Additionally, using Convolutional Neural Networks (CNNs) on imaging data has been proven to give promising results in tissue outcome prediction (Nielsen et al., 2018; Pinto et al., 2018), as well as predicting final stroke outcome (Hilbert et al., 2019). Hence, we propose two unimodal architectures based on deep learning methods: a 3D CNN to process neuroimaging data and an MLP for processing clinical metadata; both tailored

---

[a] https://orcid.org/0000-0003-2288-2406

[b] https://orcid.org/0000-0002-7936-6958

[c] https://orcid.org/0000-0001-6462-3248

[1]The code for this project can be found here: https://github.com/prediction2020/multimodal-classification

to the requirements of the data and the final outcome prediction task.

Our motivation for this work is that the fusion of multiple data modalities that observe the same phenomenon may allow for more robust predictions by capturing complementary information. Recently, using brain imaging data together with clinical information has become a popular target to replace the current time-window approach. There are several models that combine information from clinical and neuroimaging data to create a joint feature space (Cui et al., 2018; Dharmasaroja and Dharmasaroja, 2012; Johnston et al., 2002). However, these methods are limited to the manual extraction of predetermined features from brain images and therefore do not have the capacity to account for data-driven features. To the best of our knowledge, the pilot study conducted by Bacchi et al. is the only data-driven multimodal architecture developed so far that combines clinical and imaging information to predict stroke outcome.

There are mainly two types of multimodal fusion in multimodal machine learning: feature-level and decision-level. Feature-level fusion integrates features extracted from various modalities, whereas in decision level fusion the integration is performed on the final decisions of each modality. Feature-level fusion is widely used by researchers due to 1) the possibility to exploit the correlation and interactions between low level features of each modality and 2) the increasing popularity of deep learning methods for feature extraction (Poria et al., 2017; Baltrusaitis et al., 2019). In this paper we consider two strategies of feature-level fusion: extracted features and end-to-end. Most existing research on feature-level fusion adopts the extracted features strategy, where separate learning of modality features is followed by learning from the combined feature space (Wang et al., 2017; Oramas et al., 2017; Slizovskaia et al., 2017; Mouzannar et al., 2018; Kim and McCoy, 2018). However, Goh et al. point out that these existing models operate primarily on different streams of synchronous raw data (e.g. a video stream and its corresponding audio stream, or an image and its respective text caption), whereas for clinical and imaging data this synchronization does not exist. Recent work in the medical domain showed that the end-to-end strategy involving simultaneous learning of imaging and clinical modalities yielded promising results both for the diagnosis of Alzheimer's disease (Esmaeilzadeh et al., 2018) and the prediction of stroke outcome (Bacchi et al., 2019). These end-to-end studies, however, do not compare their method to the widely used extracted features approach in literature. Here, we conduct a comparative study to explore the advan-

tages and disadvantages of these two feature-level fusion approaches, i.e extracted features and end-to-end, with regards to stroke outcome prediction.

In this comparative study we use the CNN and MLP unimodal architectures (mentioned above) as fundamental building blocks, we propose two multimodal feature-level fusion strategies: 1) an extracted features strategy where the unimodal architectures are trained separately and then frozen and fused at the extracted feature-level, and 2) an end-to-end strategy where the unimodal architectures are fused at the feature-level and then trained simultaneously.

In this paper we address two research questions: (a) does the fusion of clinical and neuroimaging modalities aid in the prediction of stroke outcome, and (b) which fusion strategy is better suited for the task and data at hand.

2 DATA

The data used in this project was of patients from the 1000Plus study (Hotter et al., 2009). Examinations on patients at admission included National Institute of Health Stroke Scale (NIHSS) scoring and stroke MRI including time-of-flight (TOF) magnetic resonance angiography (MRA). TOF-MRA imaging enables the analysis of the anatomy of blood vessels, which may provide an important measure for better understanding of the vessel status and blood flow throughout the vasculature. Modified Rankin Scale (mRS), that quantifies the degree of disability or dependence in daily activities, was rated 90 days after symptoms onset. The available database consisted of 514 patients and additionally included information on patients' demographics and medical history. Of these 106 were excluded due to missing mRS score and 92 were excluded due to missing or distorted acute TOF-MRA imaging.

2.1 Clinical Data

The following seven clinical predictors were selected as clinical input: age, sex, initial NIHSS, cardiac history, diabetes, hypercholesterolemia, and thrombolysis treatment. Inclusion criteria were for categorical predictors to have at least 1 to 4 ratio of absence / existence and for all predictors to have no more than 5% missing values. Table 1 gives a summary of the clinical predictors and their distribution.

Missing values were imputed using mean imputation. The continuous variables (age, NIHSS) were centered over patients using zero-mean unit-variance.

Table 1: Statistics of clinical predictors. IQR: interquartile range; NIHSS: National Institutes of Health Stroke Scale.

Clinical information	Value
Median age (IQR)	72.0 (16.0)
Median initial NIHSS (IQR)	3.0 (4.0)
Sex (females/males)	116 / 197
Thrombolysis treatment (yes/no)	58 / 255
Cardiac history (yes/no)	87 / 226
Diabetes (yes/no)	84 / 229
Hypercholesterolemia (yes/no)	187 / 126

2.2 Imaging Data

3D volumes of acute TOF-MRA images in NIfTI format were used as imaging input[2]. The scans were gray-scale with voxel intensity values [0,255]. Figure 1 shows an example image. Images were resized from 312x384x127 to 156x192x64 voxels due to memory constraints. After resizing, the voxel intensity values were centered using zero mean and unit variance.
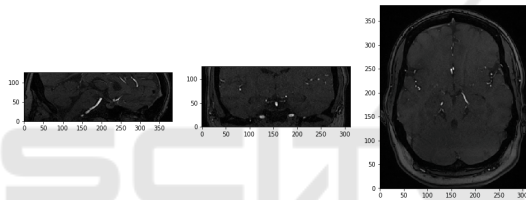

Figure 1: The middle slices of a time-of-flight magnetic resonance angiography (TOF MRA) image taken from the (A) sagittal (B) coronal and (C) horizontal planes.

3 ARCHITECTURE

All frameworks were trained on a binary classification task using binary cross-entropy loss. A softmax output layer consisting of two fully connected (FC) neurons was used as output.

3.1 Unimodal Frameworks

In the scope of this project, the unimodal frameworks were designed to 1) provide baseline performance in order to assess the value in multiple modality integration and 2) extract separately trained clinical and imaging features (Figure 3A-3B).

---

[2]All imaging is performed with a 3T MRI scanner (Tim Trio; Siemens AG, Erlangen, Germany) dedicated to clinical research. TOF vessel imaging had the following parameters: repetition time (TR) = 22 ms; echo time (TE) = 3.86 ms; time of acquisition = 3:50 minutes.

3.1.1 Multilayer Perceptron

The clinical data was modeled using a multilayer perceptron (MLP) with a single fully connected (FC) hidden layer. The number of neurons in the hidden layer was fine tuned during model selection (see section 4.2). The hidden layer neurons were rectified linear units (ReLUs). In order to prevent over-fitting 1) ℓ_2 norm regularization was introduced to penalize weights in the hidden and output layer neurons and 2) dropout was used on the hidden layer neurons.

3.1.2 Convolutional Neural Network

The 3D imaging data was modeled using a 3D convolutional neural network (CNN) consisting of three convolutional blocks followed by a single FC layer. A convolutional block refers to a set of consecutive convolutional and max pooling layers. The architecture of the CNN framework is given in Figure 2.
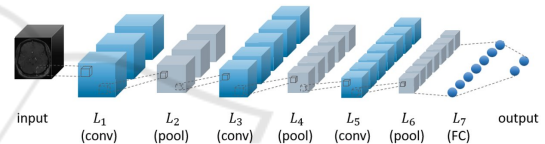

Figure 2: Illustration of the convolutional neural network used in this paper. The architecture consists of three convolutional (L_1, L_3, L_5) and three max pooling (L_2, L_4, L_6) layers followed by a fully connected (L_7) layer.

Filter size, filter stride and pooling size as well as number of filters in the convolutional layers and number of neurons in the FC layer were fine tuned during model selection (see section 4.2). All convolutional layer neurons as well as all FC layer neurons were ReLUs. ℓ_2 norm regularization was introduced to penalize weights in the convolutional and FC layers. Dropout was used only on the FC layer neurons.

3.2 Multimodal Frameworks

We developed two multimodal frameworks that have the same architectural design: In each unimodal pipeline, the output layer was dropped and the penultimate layer output was fed into an FC layer. This embedded the high dimensional imaging data into a lower dimension and vice versa for the clinical data. The outputs from these embeddings were then concatenated and fed to a final FC layer followed by the output layer (Figure 3C-3D).

The embedding layers allow for weighting of feature vectors from the two data modalities. This is done by adjusting the number of neurons in each embedding layer. For both multimodal frameworks, two
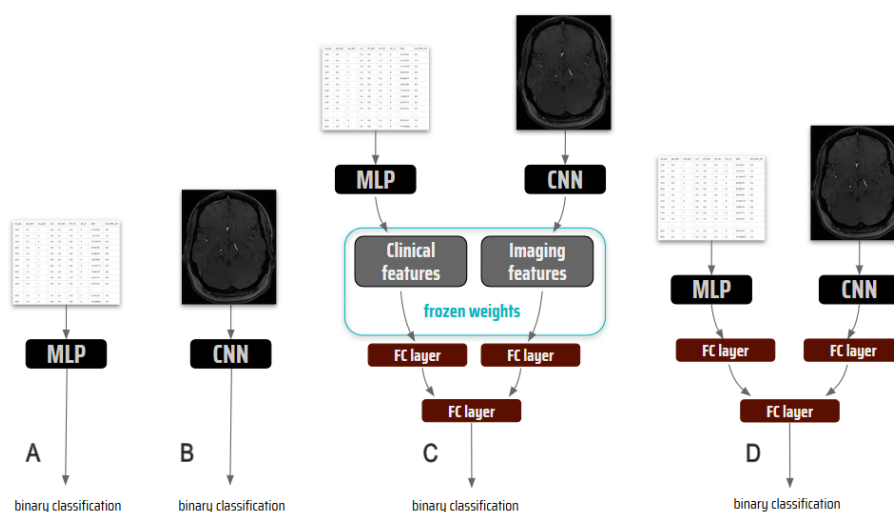
Figure 3: The frameworks: (A) Multilayer Perceptron (MLP) for modeling clinical data, (B) Convolutional Neural Network (CNN) for modeling imaging data, (C) Extracted features and (D) End-to-end strategies for modeling multimodal data.

schemes for assigning the number of neurons for feature embedding were tested: 1) assigning equal number of neurons to each modality and 2) assigning double the number of neurons for clinical feature embedding. The second scheme was chosen based on the unimodal results indicating better performance of the clinical data-based model, i.e MLP. While the architectural designs were the same for both fusion strategies, they differed in the training process.

3.2.1 Extracted Features Strategy

In this framework, the clinical and imaging features are first learned separately. The whole framework is then trained using the learned features as input, i.e the weights in the penultimate layers of the trained CNN and MLP are frozen and only the following FC layers are trained. All FC layer neurons were ReLUs. ℓ_2 norm regularization and dropout was introduced in the FC layers for regularization. The number of neurons in the embedding layers and the final FC layer were fine tuned during model selection (section 4.2).

3.2.2 End-to-End Strategy

In this strategy, the whole framework was trained end-to-end on both data modalities simultaneously (Figure 3.D), i.e the two modalities were trained together on the prediction task. All convolutional layer and all FC layer neurons were ReLUs. ℓ_2 norm regularization was used in the convolutional and FC layers, whereas dropout was only used on the FC layer neurons. The process for setting the filter size, filter stride, pooling size and number of filters of the CNN part is described in section 4.2.2. We chose a filter size of $(3x3x3)$,

filter stride of $(1x1x1)$, pooling size of $(3x3x3)$ and number of filters of $L_1 : 16, L_3 : 32, L_5 : 64$ followed by a FC layer of $L_7 : 128$ neurons (see Figure 2 for architecture). The number of neurons in the MLP hidden layer, the embedding layers and the final FC layer were fine tuned during model selection (section 4.2).

4 EXPERIMENTAL SETUP

Supervised machine learning methods were used to predict 90 days post-stroke mRS scores. The mRS range of [0,6] was dichotomized, consistently with the standard applied models in the field (Heo et al., 2019; Wouters et al., 2018). A score between [0-2] indicates good outcome (87 patients) and [3-6] indicates bad outcome (226 patients). All frameworks were trained for the same binary classification task [3].

4.1 Model Training

Binary cross-entropy loss, which quantifies how different two probability distributions are, was selected as the loss function, as it is a common choice for binary classification tasks. Loss was minimized using the Adaptive Moment Estimation (Adam) optimizer.

---

[3]All frameworks were developed using Python (v3.6.5) and all models were trained using Keras (v2.2.4) running on a Tensorflow (v1.12.0) backend. Nibabel (v2.3.0) library was used for reading imaging data and Scikit-learn (v0.20.3) library was used for pre-processing both clinical and imaging data. All training and evaluation was done on a workstation with Intel®Core™ i7-6950X CPU @ 3.00GHz x 20 and TITAN RTX GPU x 2.

Adam was recently recommended to be used as the default optimization algorithm in deep learning because of its fast convergence (Ruder, 2016). Initial weights were sampled from a Glorot uniform distribution. A Softmax function was used as the output layer activation to calculate the final class probabilities of the good and bad outcome classes.

Early stopping was introduced during training in order to prevent over-fitting: training stopped once the improvement in validation loss was below a specified value. The value for each framework was set depending on the appropriate range of the validation loss.

4.2 Model Selection

In addition to the architectural hyper-parameters selected in each framework for fine tuning (sections 3.1 and 3.2) the following hyper-parameters were fine tuned: batch size, ratio of the ℓ_2 norm regularization, dropout rate and the learning rate of the optimizer.

4.2.1 Training-validation-test Splits

The data was randomly split into three subsets: training, validation and test with 200, 50 and 63 patients in each respectively. Patients in each set corresponded for both input modalities, i.e. the clinical and imaging information in each set was from the same patients. Additionally, the sets were consistently used for training, validation and testing of each of the four frameworks, in order to achieve comparable results.

To account for the variance between subsets, which is likely to be higher in small datasets, the random selection of training-, validation- and test sets was repeated five times resulting in five different

splits. Model selection using grid search was therefore repeated for each split. This aims to reduce bias and variance of the models. Since grid search resulted in different hyper-parameters in different splits, final performance was assessed for each split individually.

4.2.2 Grid Search

Model selection, i.e the best choice of hyper-parameters, was done using an exhaustive search method called grid search. Using grid search, models were trained and evaluated on the training and validation sets respectively for each hyper-parameter combination. The hyper-parameter combination that yielded best model performance on the validation set were chosen for final training. Model performance on the validation set was evaluated using area under the receiver operator characteristics curve (AUC) score. Typically the cross-validation method is used to overcome variance in model performance; however, due to computational limitations (e.g. long training times) it was not adopted in this project. Finally, using the selected hyper-parameters a final model was trained on the combined training and validation data. The same model selection process was carried out for all five training-validation-test splits, resulting in five models for each framework.

The only exception to this model selection process was the CNN in the end-to-end fusion framework. In order to save computational power and time, rather than fitting the architecture hyper-parameters (filter size, filter stride, pooling size and number of filters) as part of a grid search, they were pre-set to the most frequently occurring combination of these hyper-parameters found across the five splits of fitting the unimodal CNN architecture.

Table 2: (a) Test and (b) training performances by median and interquartile range (IQR) calculated over 100 training and test runs. Columns represent the different splits, last column shows the average over the other five. Rows represent the 1) convolutional neural network (CNN), 2) multilayer perceptron (MLP), 3) feature extraction and 4) end-to-end frameworks.

(a) Test performance

Framework	median AUC score (iqr)					
	Split 1	Split 2	Split 3	Split 4	Split 5	Splits average
CNN	0.61 (0.05)	0.76 (0.03)	0.68 (0.03)	0.68 (0.04)	0.67 (0.2)	0.68
MLP	0.70 (0.05)	0.76 (0.02)	0.80 (0.01)	0.71 (0.06)	0.78 (0.05)	0.75
Extracted features	0.60 (0.02)	0.78 (0.01)	0.78 (0.02)	0.76 (0.01)	0.83 (0.01)	0.75
End-to-end	0.71 (0.04)	0.78 (0.02)	0.79 (0.03)	0.73 (0.05)	0.81 (0.04)	0.76

(b) Training performance

Framework	median AUC score (iqr)					
	Split 1	Split 2	Split 3	Split 4	Split 5	Splits average
CNN	0.97 (0.04)	0.99 (0.004)	1.00 (0)	0.94 (0.08)	0.89 (0.3)	0.96
MLP	0.81 (0.05)	0.85 (0.01)	0.87 (0.004)	0.82 (0.03)	0.83 (0.03)	0.84
Extracted features	0.97 (0.004)	0.96 (0.006)	0.99 (0.001)	0.88 (0.007)	0.99 (0.001)	0.96
End-to-end	0.90 (0.06)	0.90 (0.07)	0.91 (0.06)	0.92 (0.08)	0.87 (0.08)	0.90

4.3 Model Evaluation

Model performances were measured using AUC. To evaluate overfitting, the AUC score was calculated on both the respective training (merged training and validation sets) and test sets of the trained models.

Variations in model performance due to random processes such as dropout and parallel computing was investigated by repeated training and evaluation. The repetition was 100 times for each training-validation-test split. The median and interquartile range (IQR) over the 100 training and test AUC scores was calculated and used as the final performance measure. Additionally, variation in model performance due to data variability was investigated by calculating the mean AUC score over the median of five splits.

Finally, a non-parametric paired t-test, i.e. Wilcoxon signed rank test, was performed in order to determine if the multimodal frameworks (i.e. end-to-end and feature extraction) significantly outperformed the clinical data driven MLP network. The test was based on the distribution of test performances given by the 100 runs within each split. Here, multimodal frameworks were compared to the clinical data based MLP framework in order to highlight the benefits of integrating neuroimaging information.

5 RESULTS

Table 2 summarizes performances for the unimodal and multimodal frameworks. For each split, median AUC scores calculated over 100 training and evaluation runs are presented together with the IQR. Average training and test performance over splits (calculated as the mean) is given in the last column.

Imaging. CNN showed low performance on the test sets with a mean AUC score of 0.68 over the splits, but performed very high on the training sets with a mean AUC score of 0.96 This result indicates a strong overfitting in the CNN models.

Clinical. MLP performed well on both the training and test sets with an average AUC score of 0.84 and 0.75 respectively. The MLP was therefore less prone to overfitting compared to the CNN.

Multimodal. The feature extraction framework performed on average the same as the MLP framework and better than the CNN frameworks with an AUC of 0.75 on test sets. On the other hand, performance on the training sets reached an average of 0.96, the same value as the CNN models average. In general

the feature extraction framework was the most stable in both training and test performances with an IQR of no more than 0.02 on any of the splits.

The end-to-end framework performed better than the MLP on average in both training and test sets with AUC scores of 0.90 and 0.76 respectively. Additionally end-to-end performed better than the CNN only in average test performance, thus not exhibiting the overfitting characteristic of the CNN.

Significance. Table 3 shows the results of the Wilcoxon signed rank test that was based on the distribution of test performances within each split. The significance test showed that the end-to-end framework performed significantly better compared to the clinical based MLP framework in all splits with the exception of split 3, which showed the opposite result. The feature extraction framework yielded inconsistent results, with significantly improved performance for 3 of the splits (i.e. 2,4,5) and significantly worse performance for the other two splits.

6 DISCUSSION

Our results show that there is potentially clinical value in TOF-MRA images for stroke outcome prediction. Both multimodal architectures displayed better test performance in the majority of the five splits compared to the MLP and CNN models trained only on clinical and neuroimaging data respectively.

Of the two multimodal feature-level fusion strategies, the end-to-end strategy achieved more consistent improvement over the five splits. Although the improvements were not substantial, they were shown to be statistically significant by the Wilcoxon signed rank test. On the other hand, while showing a lower averaged performance over splits, the extracted features strategy demonstrated higher stability within a split, i.e a lower variance in performance over the 100 runs within a split, indicated by IQR values. This is expected, since the extracted features framework only learns the final FC layer weights, which makes this strategy less prone to variations caused by random processes during learning.

The test and training performance patterns demonstrate that the extracted features strategy enforces a strong prediction bias towards one of the modalities. This bias is well exemplified in the first split, where the effect of the low performing CNN model is reflected in the test performance of the extracted features model. Here, since the imaging features were extracted from a low performing model and were not introduced as trainable parameters in the ex-

Table 3: The Wilcoxon signed rank test p values on test performances over 100 runs. The test compares a) end-to-end against the MLP and b) extracted features against the MLP. The splits where the multimodal frameworks outperformed the unimodal MLP (in terms of median AUC score) are highlighted in bold.

Frameworks	p values				
	Split 1	Split 2	Split 3	Split 4	Split 5
Extracted features vs. MLP	7e-18	**3e-13**	6e-16	**4e-16**	**1e-17**
End-to-end vs. MLP	**5e-04**	**3e-11**	5e-03	**6e-04**	**4e-08**

tracted features framework, the inherent shortcomings of the learned imaging features could not be mitigated through additional representation learning in the MLP network. Whereas in the end-to-end framework, since the features from both modalities are extracted and learned simultaneously, the network seems to adapt itself to the better performing modality (e.g clinical metadata), hence alleviating the poor feature representation of the CNN pipeline. The same effect is expressed in the training performances of all splits. The extracted features strategy displays the near-to-perfect training performance of the CNN framework more profoundly than the end-to-end strategy. Following these findings we can suggest that the extracted features approach may be a stronger strategy when both modalities perform well for the task at hand separately, but not when one modality suffers from low performance. We show that for the case at hand, the end-to-end strategy works better.

In the scope of this project imaging data was hypothesized as a means to improve the performance of clinical-based outcome prediction models, rather than providing reliable outcome prediction by itself. Nevertheless, the CNN framework trained only on imaging data for the outcome prediction task showed comparable results to the data-efficient method of Hilbert et al., 2019. At the same time, performance was relatively high on the training sets compared with the test sets, indicating that the model was suffering from overfitting. Overfitting could not be overcome by the introduced regularization methods such as ℓ_1, ℓ_2 norm regularizations, dropout, batch normalization or decreasing number of model parameters by using less convolutional blocks or less number of filters. This shows that even when the architecture is tailored to the needs of the data and task at hand, the features discovered during training are not representative of the actual classification task but rather tailored to the correlation between the input and output of the training set. This may be resulting from the properties of the imaging data, the complexity of the model class and the coarse definition of the classification problem.

Our study has several limitations. First, the small sample size of the given cohort limits the generalizability of our models. Although many clinical predictors were recorded in the 1000Plus study, only seven predictors could be included in our project due to the high percentage of missing data. In this case, the ratio of features to sample size showed to be sufficient enough to prevent overfitting, but having more features might have been beneficial in utilizing the full capacity of a complex model, such as an MLP. Similarly for imaging, several patients had to be excluded due to incomplete scans. In this case, since every voxel in the input image is considered as a feature, the feature space was very large in comparison to the sample size. This can explain the strong overfitting behaviour of the CNN models. Additionally, a small sample size resulted in high data variability between training-validation-test sets. This was demonstrated by the performance inconsistency between splits. Furthermore, limitations in computational power restricted the training of the CNN and end-to-end to small mini-batches. Additionally since model training is longer with imaging data, cross validation was not used during model selection and the number of training-validation-test sets were limited to five. Performing cross validation for selecting the best hyper-parameters may provide more stability in overall model performances, i.e. variance between and within splits will be reduced. The same argument is valid if more training-validation-test sets can be used for model selection and evaluation. Improved stability by using cross-validation and increased number of splits may allow for a more reliable comparison between the two multimodal fusion approaches.

7 CONCLUSION

We developed and evaluated two multimodal feature-level fusion frameworks to predict final outcome in acute ischemic stroke patients using clinical data and neuroimaging. We showed that a multimodal approach achieves better results and neuroimaging may hold beneficial information for outcome prediction when used with clinical metadata. We demonstrated how a multimodal approach using simultaneous end-to-end learning of modalities, outperforms learning from the combination of separately learned features.

ACKNOWLEDGEMENTS

REFERENCES

Asadi, H., Dowling, R., Yan, B., and Mitchell, P. (2014). Machine Learning for Outcome Prediction of Acute Ischemic Stroke Post Intra-Arterial Therapy. *PLoS ONE*, 9(2):e88225.

Bacchi, S., Zerner, T., Oakden-Rayner, L., Kleinig, T., Patel, S., and Jannes, J. (2019). Deep Learning in the Prediction of Ischaemic Stroke Thrombolysis Functional Outcomes: A Pilot Study. *Academic Radiology*, pages 1–5.

Baltrusaitis, T., Ahuja, C., and Morency, L. P. (2019). Multimodal Machine Learning: A Survey and Taxonomy. *IEEE Transactions on Pattern Analysis and Machine Intelligence*, 41(2):423–443.

Cui, H., Wang, X., Bian, Y., Song, S., and Feng, D. D. (2018). Ischemic stroke clinical outcome prediction based on image signature selection from multimodality data. In *2018 40th Annual International Conference of the IEEE Engineering in Medicine and Biology Society (EMBC)*, pages 722–725. IEEE.

Dharmasaroja, P. and Dharmasaroja, P. A. (2012). Prediction of intracerebral hemorrhage following thrombolytic therapy for acute ischemic stroke using multiple artificial neural networks. *Neurological Research*, 34(2):120–128.

Esmaeilzadeh, S., Belivanis, D. I., Pohl, K. M., and Adeli, E. (2018). End-To-End Alzheimer's Disease Diagnosis and Biomarker Identification. pages 337–345.

Heo, J., Yoon, J. G., Park, H., Kim, Y. D., Nam, H. S., and Heo, J. H. (2019). Machine Learning–Based Model for Prediction of Outcomes in Acute Stroke. *Stroke*, 50(5):1263–1265.

Hilbert, A., Ramos, L. A., van Os, H. J., Olabarriaga, S. D., Tolhuisen, M. L., Wermer, M. J., Barros, R. S., van der Schaaf, I., Dippel, D., Roos, Y. B., van Zwam, W. H., Yoo, A. J., Emmer, B. J., Lycklama à Nijeholt, G. J., Zwinderman, A. H., Strijkers, G. J., Majoie, C. B., and Marquering, H. A. (2019). Data-efficient deep learning of radiological image data for outcome prediction after endovascular treatment of patients with acute ischemic stroke. *Computers in Biology and Medicine*, 115(October):103516.

Hotter, B., Pittl, S., Ebinger, M., Oepen, G., Jegzentis, K., Kudo, K., Rozanski, M., Schmidt, W. U., Brunecker, P., Xu, C., Martus, P., Endres, M., Jungehülsing, G. J., Villringer, A., and Fiebach, J. B. (2009). Prospective study on the mismatch concept in acute stroke patients within the first 24 h after symptom onset - 1000Plus study. *BMC Neurology*, 9(1):60.

Johnston, K. C., Wagner, D. P., Haley, E. C., and Connors, A. F. (2002). Combined Clinical and Imaging Information as an Early Stroke Outcome Measure. *Stroke*, 33(2):466–472.

Kelleher, J. D. (2019). *Deep Learning*. MIT Press.

Kim, E. and McCoy, K. F. (2018). Multi modal deep learning using images and text for information graphic classification. *ASSETS 2018 - Proceedings of the 20th International ACM SIGACCESS Conference on Computers and Accessibility*, pages 143–148.

Mouzannar, H., Rizk, Y., and Awad, M. (2018). Damage Identification in Social Media Posts Using Multimodal Deep Learning. *Proceedings of the International ISCRAM Conference*, 2018-May(May):529–543.

Nielsen, A., Hansen, M. B., Tietze, A., and Mouridsen, K. (2018). Prediction of Tissue Outcome and Assessment of Treatment Effect in Acute Ischemic Stroke Using Deep Learning. *Stroke*, 49(6):1394–1401.

Oramas, S., Nieto, O., Sordo, M., and Serra, X. (2017). A deep multimodal approach for cold-start music recommendation. *ACM International Conference Proceeding Series*, Part F1301:32–37.

Pinto, A., Mckinley, R., Alves, V., Wiest, R., Silva, C. A., and Reyes, M. (2018). Stroke Lesion Outcome Prediction Based on MRI Imaging Combined With Clinical Information. *Frontiers in Neurology*, 9.

Poria, S., Cambria, E., Bajpai, R., and Hussain, A. (2017). A review of affective computing: From unimodal analysis to multimodal fusion. *Information Fusion*, 37:98–125.

Ruder, S. (2016). An overview of gradient descent optimization algorithms.

Slizovskaia, O., Gomez, E., and Haro, G. (2017). Musical instrument recognition in user-generated videos using a multimodal convolutional neural network architecture. *ICMR 2017 - Proceedings of the 2017 ACM International Conference on Multimedia Retrieval*, pages 226–232.

Vora, N. A., Shook, S. J., Schumacher, H. C., Tievsky, A. L., Albers, G. W., Wechsler, L. R., and Gupta, R. (2011). A 5-Item Scale to Predict Stroke Outcome After Cortical Middle Cerebral Artery Territory Infarction. *Stroke*, 42(3):645–649.

Wang, D., Mao, K., and Ng, G.-W. (2017). Convolutional neural networks and multimodal fusion for text aided image classification. In *2017 20th International Conference on Information Fusion (Fusion)*, pages 1–7. IEEE.

Whiteley, W. N., Slot, K. B., Fernandes, P., Sandercock, P., and Wardlaw, J. (2012). Risk Factors for Intracranial Hemorrhage in Acute Ischemic Stroke Patients Treated With Recombinant Tissue Plasminogen Activator. *Stroke*, 43(11):2904–2909.

Wouters, A., Nysten, C., Thijs, V., and Lemmens, R. (2018). Prediction of Outcome in Patients With Acute Ischemic Stroke Based on Initial Severity and Improvement in the First 24 h. *Frontiers in Neurology*, 9.